

Depth3DLane: Monocular 3D Lane Detection via Depth Prior Distillation

Dongxin Lyu
Jilin University

lvdx2122@mails.jlu.edu.cn

Cheng Tan
Zhejiang University & Westlake University
tancheng@westlake.edu.cn

Han Huang
Fuzhou University, China

832201324@fzu.edu.cn

Zimu Li
Shanghai Jiao Tong University
li_zimu@sjtu.edu.cn

Abstract

Monocular 3D lane detection is challenging due to the difficulty in capturing depth information from single-camera images. A common strategy involves transforming front-view (FV) images into bird's-eye-view (BEV) space through inverse perspective mapping (IPM), facilitating lane detection using BEV features. However, IPM's flat-ground assumption and loss of contextual information lead to inaccuracies in reconstructing 3D information, especially height. In this paper, we introduce a BEV-based framework to address these limitations and improve 3D lane detection accuracy. Our approach incorporates a Hierarchical Depth-Aware Head that provides multi-scale depth features, mitigating the flat-ground assumption by enhancing spatial awareness across varying depths. Additionally, we leverage Depth Prior Distillation to transfer semantic depth knowledge from a teacher model, capturing richer structural and contextual information for complex lane structures. To further refine lane continuity and ensure smooth lane reconstruction, we introduce a Conditional Random Field module that enforces spatial coherence in lane predictions. Extensive experiments validate that our method achieves state-of-the-art performance in terms of z-axis error and outperforms other methods in the field in overall performance. The code is released at: <https://anonymous.4open.science/r/Depth3DLane-DCDD>.

1. Introduction

Monocular 3D lane detection has become essential in autonomous driving due to its efficiency and cost-effectiveness compared to more complex sensor setups. Accurate 3D lane detection provides critical information for vehicle localization, navigation, and route planning, making it a foundational component for advanced driver assis-

tance systems. However, the inherent challenge of estimating depth from a single image poses significant obstacles, as monocular setups struggle to provide accurate spatial information without the depth cues available in multi-camera or sensor-based systems.

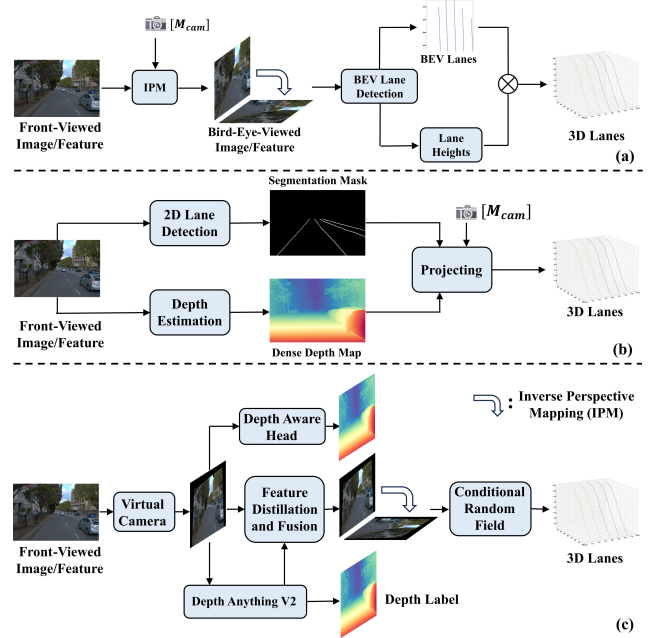


Figure 1. (a) BEV-based methods convert front-view images to BEV for lane detection; (b) Non-BEV methods project 2D lanes into 3D using depth estimation; (c) The proposed Depth3DLane framework combines Hierarchical Depth-Aware Head, Feature Distillation and Fusion, and a Conditional Random Field (CRF) for coherent 3D lane predictions.

A variety of methodologies have emerged to tackle this challenge, which is illustrated in Figure 1. For example, BEV-LaneDet [33] employs a Virtual Camera that transforms front-view images into a consistent BEV represen-

tation to ensure spatial consistency, adapting effectively to complex scenarios through a keypoint-based representation of 3D lanes. Similarly, GroupLane [19] introduces a classification strategy within the bird’s-eye view (BEV) framework, accommodating lanes in multiple orientations and enabling the interaction of feature information across instance groups. CurveFormer [2] utilizes sparse query representations and cross-attention mechanisms to effectively regress the polynomial coefficients of 3D lanes. Building upon this groundwork, LATR [22] develops lane-aware query generators and dynamic 3D positional embeddings. Furthermore, CurveFormer++ [3] proposes a single-stage detection method that bypasses the need for image feature view transformations, facilitating direct inference from perspective images.

Despite these advances, accurately estimating lane height from monocular images remains challenging. The complexity of reconstructing the third dimension from a single front-view (FV) image complicates this task, as accurate height estimation relies heavily on depth information, which reflects the distance from the camera to objects in the scene [11, 13, 22]. Existing approaches often rely on model architectures to extract height information but face difficulties due to the absence of well-structured labels designed explicitly for height estimation [2, 5, 7, 8, 21, 33]. Alternative approaches include direct regression [17], weakly supervised learning using 2D labels [1], as well as employing LiDAR [24] and other multi-modal techniques to gather and fuse height data. However, these methods either introduce higher equipment and computational costs or fail to achieve precise prediction results.

Our inspiration stems from Depth Anything V2 [35], which leverages synthetic data to train a teacher model that generates pseudo-labels for training a student model, offering reliable depth priors without the need for expensive depth annotations. As shown in Figure 1, this approach enables the accurate and robust estimation of the depth distribution from input monocular images. **Building upon this foundational motivation, we propose three main contributions in this work:**

1. *Hierarchical Depth-Aware Head:* Inspired by the U-Net architecture [26], we design a specialized head to facilitate depth feature learning, significantly improving the model’s capability in perceiving spatial relationships and extracting 3D lane features.
2. *Feature Distillation and Fusion:* Utilizing Depth Anything V2 [35] as a pretrained teacher model, we distill depth-aware features into student models, which are then fused into corresponding feature layers, significantly enhancing height estimation and 3D spatial representation.
3. *Prior Knowledge and CRF Integration:* Leveraging priors on the relative invariance of lane appearances and uniform depth variations, we employ a *Conditional Ran-*

dom Field [15] to refine output predictions, further enhancing accuracy and robustness.

2. Related Work

2D Lane Detection. Recent advancements in 2D lane detection have leveraged a variety of deep learning methodologies, categorized into segmentation-based, anchor-based, keypoint-based, and curve-based approaches [23]. Segmentation-based techniques focus on pixel-wise classification [12, 20], generating comprehensive lane masks but often incurring high computational costs. Researchers have improved real-time capabilities within this framework while maintaining accuracy. Conversely, anchor-based methods [18, 28, 36] enhance efficiency by utilizing predefined anchor points for lane estimation; however, they struggle with intricate lane configurations. Keypoint-based techniques [14, 25, 31] have emerged to model lane detection as sparse keypoint estimation, providing adaptability to complex lane geometries, albeit with challenges related to maintaining lane continuity. In contrast, curve-based methods [20, 29, 30] utilize polynomial or curve regression, transforming the detection task into a parameter regression problem. While effective in structured environments, these methods often require additional transformations like inverse perspective mapping (IPM), which can restrict their application across diverse terrains.

3D Lane Detection. Meanwhile, research on 3D lane detection has gained significant traction by leveraging the benefits of depth information from monocular images [23]. The transition from 2D to 3D lane detection addresses the limitations of depth ambiguity inherent in 2D methods, a crucial advancement for applications in autonomous driving. Early monocular 3D lane detection methods, such as 3D-LaneNet [7] and Gen-LaneNet [8], introduced anchor-based representations to estimate lane depth, using techniques like intra-network IPM for multi-view consistency. PersFormer [5] extends these ideas by integrating Transformer-based spatial transformations, thereby enhancing feature robustness across complex perspectives and introducing the OpenLane dataset, which has become a cornerstone resource in 3D lane detection research.

Recent approaches have evolved to incorporate CNN and Transformer architectures for better feature mapping and depth accuracy in challenging scenes. Anchor3DLane [11] utilizes a BEV-free framework to directly predict 3D lane points from front-view features, bypassing the need for additional transformations. On the other hand, Transformer-based approaches, such as LATR [22] and CurveFormer [2], leverage attention mechanisms and dynamic query generation to iteratively refine lane representations, effectively handling complex lane geometries without the need for explicit BEV transformations. Furthermore, a keypoint-based approach called BEV-LaneDet [33] further advances the

field by offering a straightforward and effective baseline for 3D lane detection. This approach introduces a *Virtual Camera* to project images to a standardized view, maintaining spatial consistency across frames. We adopted the concept of a *Virtual Camera* to standardize all input camera extrinsic and intrinsic parameters, thereby eliminating ambiguities. While keypoint-based methods typically exhibit better fitting performance, they may not perfectly conform to curved shapes. To address this limitation, we propose a keypoint-based approach that utilizes *Conditional Random Fields* to integrate lane line prior knowledge, thereby refining the model’s output.

Monocular Depth Estimation (MDE). Height reconstruction is one of the key advancements that differentiates 3D lane detection from its 2D counterpart. However, the limitations of monocular data make this particularly challenging. As a result, MDE has provided significant support for Monocular 3D lane detection, offering a cost-effective alternative to LiDAR systems. M4Depth [6] utilizes a single moving camera to create disparity maps from motion, improving depth estimation in unfamiliar environments. Enhancing self-supervision, DaCCN [9] avoids extensive labeled data by leveraging direction-aware modules, thus refining depth without costly sensors. Bavirisetti et al. [4] proposed a new approach to integrate depth estimation with semantic segmentation, enriching object identification and spatial awareness for real-time navigation. Further advancing MDE, Depth Anything [34] predicts depth maps from a single image using a CNN-based encoder-decoder architecture trained on large-scale datasets to enhance generalization. Depth Anything V2 [35] improves upon this by incorporating attention mechanisms and multi-task learning, which increase accuracy and robustness in depth estimation. Drawing inspiration from these significant advancements, our work integrates insights from the pretrained depth estimation model, particularly Depth Anything V2. By utilizing the learned knowledge of monocular depth estimation from this pretrained model, our approach significantly enhances the effectiveness of lane detection.

3. Methodology

The overall architecture of the proposed Depth3DLane is depicted in Figure 2. Given an input image $\mathbf{I} \in \mathbb{R}^{H \times W \times 3}$, we first normalize its in/extrinsic parameters to ensure consistency using the *Virtual Camera* [33]. Next, we design the *Hierarchical Depth-Aware Head*, an encoder-decoder architecture that extracts depth-related features with enhanced spatial understanding. To further improve spatial awareness and uniformity, we employ *Feature Distillation and Fusion* process, transferring knowledge from two transformer layers of a teacher model, *Depth Anything V2* [35], to two corresponding feature scale layers. This results in two hierarchical feature maps that capture multi-scale depth informa-

tion.

These front-view feature maps are then projected into Bird’s Eye View (BEV) features using a *Spatial Transformation Pyramid* (STP)—a lightweight, multi-scale spatial transformation module. Before making the final lane predictions, we integrate a *Conditional Random Field* to enhance lane continuity and robustness. The *Conditional Random Field* leverages pairwise potentials $p(x_i, x_j)$, ensuring consistent labeling for adjacent pixels with similar color and depth properties, thus reducing noise and improving structural coherence. Finally, we project the detected lane onto the road plane P_{road} , which corresponds to the plane where $z = 0$ in road-ground coordinates, denoted as $C_{\text{road}} = (x, y, z)$.

3.1. Hierarchical Depth-Aware Head

To efficiently leverage depth information and address the limitations of IPM-based methods, we introduce the *Hierarchical Depth-Aware Head*, a U-Net-inspired [26] module integrated with the ResNet [10] backbone. Designed as an encoder-decoder structure, this module provides multi-scale depth guidance to mitigate two main IPM issues: the flat-ground assumption, which fails on slopes, and the loss of height and contextual information above the road surface [11]. By refining depth predictions at multiple levels, the *Hierarchical Depth-Aware Head* captures 3D spatial information beyond the ground plane, adding minimal complexity during training and no cost at inference. The *Hierarchical Depth-Aware Head* includes:

- **Encoder Path:** Mirrors the backbone’s hierarchical feature extraction, capturing depth-related features across scales to adapt to varied ground conditions and improve 3D lane localization.
- **Auxiliary Decoder Path:** Uses upsampling and convolutional layers to progressively reconstruct depth maps during training, offering auxiliary supervision to enhance depth feature learning. The decoder is active only in training, ensuring real-time efficiency at inference.

The multi-scale depth guidance is formalized as:

$$D = \text{Decoder}(\text{Encoder}(F_{\text{backbone}})) \quad (1)$$

where F_{backbone} is the feature map from the ResNet [10] backbone, Encoder and Decoder represent the U-Net [26] paths, and D is the refined depth map for auxiliary supervision. By refining depth predictions at various levels during training, the *Hierarchical Depth-Aware Head* effectively preserves height and contextual information, enabling accurate 3D lane localization across varied road geometries.

3.2. Feature Distillation and Fusion

The *Feature Distillation and Fusion* component is central to the methodology of the Depth3DLane framework, enabling effective depth knowledge transfer from a pre-trained

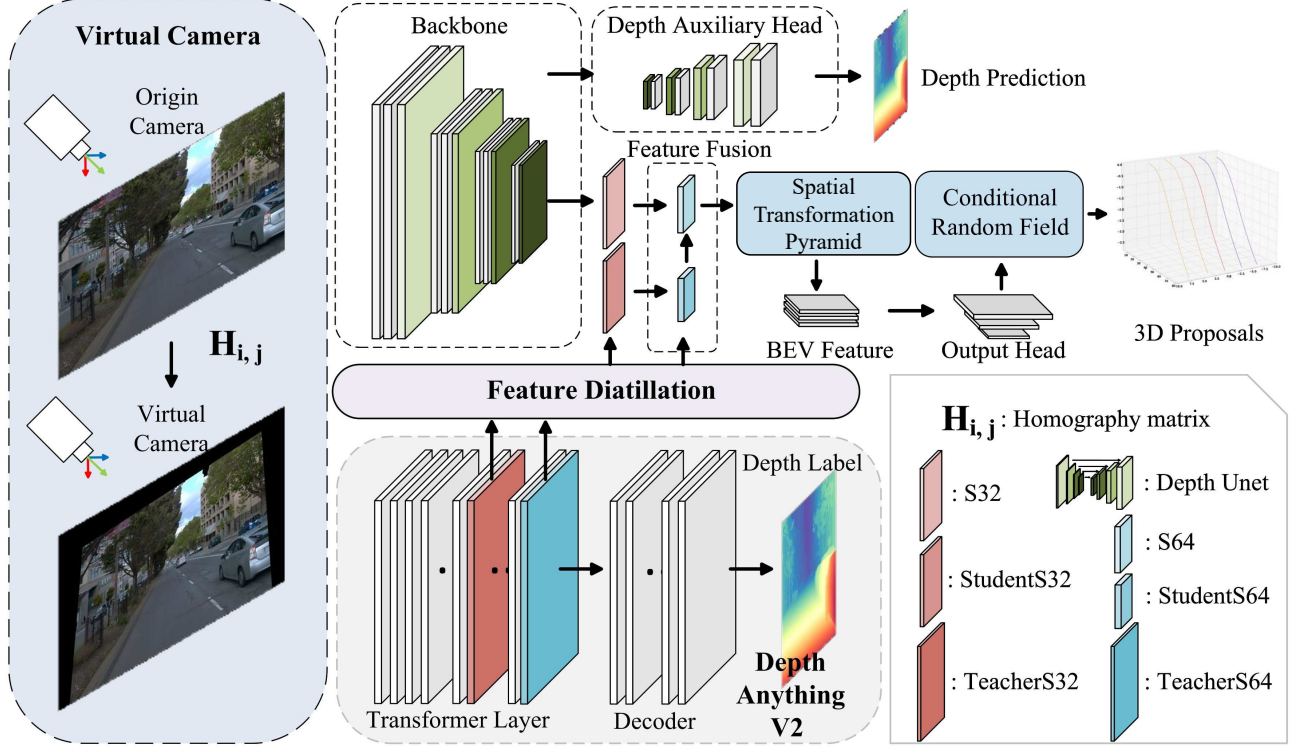


Figure 2. Overview of the proposed Depth3DLane framework. First, input images from diverse viewpoints are standardized into a unified perspective using a *Virtual Camera* [33]. Next, a ResNet backbone [10] extracts essential front-view features, followed by multi-scale depth extraction via the proposed *Hierarchical Depth-Aware Head*. Meanwhile, depth knowledge is distilled from a pretrained Depth Anything V2 [35] into student modules (StudentS32 and StudentS64), and subsequently aligned and fused with corresponding backbone features. Finally, the enriched features undergo BEV transformation through a *Spatial Transformation Pyramid* and refinement by a *Conditional Random Field* module, producing robust and coherent 3D lane predictions.

teacher model, Depth Anything V2 [35] to the student models, StudentS32 and StudentS64. This process is designed to enhance the STP’s feature extraction capabilities by aligning and refining feature maps across multiple spatial resolutions, ultimately improving the model’s 3D lane detection performance.

In feature distillation, the student models are trained to replicate the feature representations of the teacher model, Depth Anything V2 [35], at their respective resolutions (S32 and S64). To capture rich semantic information, we select layer17 and layer23 from Depth Anything V2, as these deeper encoder layers effectively represent high-level abstractions crucial for complex lane detection. StudentS32, associated with layer17, refines high-resolution feature maps to detect intricate lane boundaries, while StudentS64, linked to layer23, focuses on lower-resolution feature maps to encapsulate broader spatial context. This hierarchical arrangement ensures that StudentS32 and StudentS64 complement each other by learning from distinct semantic levels, resulting in a comprehensive feature representation that strengthens the Depth3DLane framework’s

3D lane detection performance.

Following the distillation process, the refined features from the student models, denoted as $\mathbf{F}_{\text{distilled}}$, are fused with the STP’s lower-resolution feature maps, represented by \mathbf{F}_{STP} . This fusion is achieved through the concatenation operation (Concat) along the channel dimension:

$$\mathbf{F}_{\text{fused}} = \text{Concat}(\mathbf{F}_{\text{STP}}, \mathbf{F}_{\text{distilled}}) \quad (2)$$

By leveraging the rich feature hierarchies learned by the teacher model, feature distillation enables improved feature quality and generalization without significant model complexity increase. Moreover, combining distilled depth features with the *Hierarchical Depth-Aware Head* enhances spatial accuracy through complementary interactions. Consequently, this approach contributes to efficient training dynamics and robust 3D lane detection within the DepthLane framework.

3.3. Conditional Random Field

In keypoint-based 3D lane detection models, one of the challenges lies in the potential misalignment of predicted

keypoints, leading to incomplete or fragmented lane shapes that cannot be seamlessly reconstructed into a continuous curve [32]. This issue arises due to the discrete nature of keypoint predictions, where gaps between adjacent points may result in non-smooth or disconnected lane segments. To address this problem, we used a *Conditional Random Field* module to refine the output from Depth3DLane.

In lane detection models, the prediction error for lane lines that are closer to the camera is typically much smaller than for those farther away. To address this discrepancy, we define the baseline pixel of the i -th lane as the pixel located at the bottom center of the lane in the predicted image. This baseline pixel serves as a reference point for the i -th lane line. To reduce unnecessary computations and mitigate the influence of irrelevant pixels, we propose constructing an independent *Conditional Random Field* for each lane line. Specifically, a separate *Conditional Random Field* is initiated from the baseline pixel of each lane, ensuring a more efficient and localized optimization process.

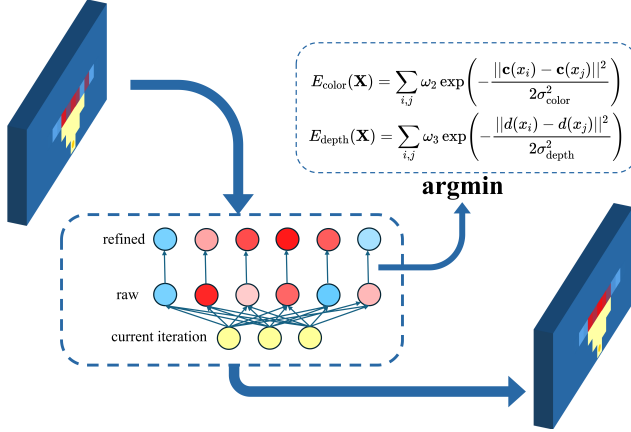


Figure 3. End-to-End abstract structure figure

For a prediction matrix from model \mathbf{X} where x_i represents the i -th pixel

$$E(\mathbf{X}) = \sum_i \omega_1 u(x_i) + \sum_{i,j} p(x_i, x_j). \quad (3)$$

The unary potential term $u_{x_i} = -\log P(x_i)$ considers the predicted probability $P(x_i)$ from the Depth3dLane model. The pairwise potential term.

The pairwise potential in our work consists of two components: color and depth potentials. We use Gaussian kernels to calculate their energies

$$\begin{aligned} p(x_i, x_j) &= \omega_2 p_{color}(x_i, x_j) + \omega_3 p_{depth}(x_i, x_j) \\ &= \omega_2 \exp\left(-\frac{\|\mathbf{c}(x_i) - \mathbf{c}(x_j)\|^2}{2\sigma_{color}^2}\right) \\ &\quad + \omega_3 \exp\left(-\frac{\|d(x_i) - d(x_j)\|^2}{2\sigma_{depth}^2}\right). \end{aligned} \quad (4)$$

The color potential p_{color} depends on the color distance between adjacent pixels $\mathbf{c}(i) - \mathbf{c}(j)$ where $\mathbf{c}(i)$ denotes the color vector of pixel i . The depth potential p_{depth} depends on the output from Depth Anything V2 [35] model.

4. Experiments

4.1. Datasets and Evaluation Metrics

To evaluate the effectiveness of our work, we conduct experiments on two widely recognized datasets: Apollo Synthetic[8] and OpenLane[5].

Apollo Synthetic is a synthetic dataset generated using the Unity 3D engine. It provides photorealistic images across different driving environments such as highways, urban streets, and residential areas. The dataset is particularly useful for controlled testing, with variations in lighting, weather, and road surface conditions, enabling a detailed assessment of lane detection algorithms under a wide array of simulated conditions.

OpenLane, on the other hand, is a large-scale, real-world dataset derived from the Waymo Open Dataset[27], consisting of 200,000 frames and over 880,000 annotated lanes. This dataset offers a diverse range of scene metadata, including weather conditions and geographical locations, ensuring a comprehensive evaluation across various environmental factors.

Evaluation Metrics. For evaluation on both 3D datasets, we use the metrics proposed by Gen-LaneNet [8], which encompass F-Score across different scenes and X/Z errors in various regions. We adopt standard metrics widely used in 3D lane detection research.

4.2. Comparison Studies

We compare Depth3DLane with recent state-of-the-art methods, including 3D-LaneNet [7], Gen-LaneNet [8], PersFormer [8], Anchor3DLane [11], and BEV-LaneDet [33]. Evaluation is performed on both OpenLane and Apollo 3D Synthetic datasets under diverse driving conditions, including curved roads, uphill/downhill gradients, and extreme weather scenarios.

4.2.1. Results on Apollo 3D Synthetic

As presented in Table 1, our model demonstrates strong overall accuracy with an AP of 97.7% in the balanced scene, slightly outperforming leading methods such as BEV-LaneDet [33] and Anchor3DLane [11]. The F1 score of 98.9% further illustrates the precision and recall stability achieved by Depth3DLane. Importantly, Depth3DLane achieves the lowest z-axis localization error in the far range (z-Err/F) of 0.201m, a notable improvement compared to other methods, emphasizing its effectiveness in distant lane detection.

In the rare subset, our model displays its robustness in complex and infrequent lane configurations. Depth3DLane

Scene	Method	AP(%)↑	F1(%)↑	x-Err/N(m)↓	x-Err/F(m)↓	z-Err/N(m)↓	z-Err/F(m)↓
Balanced Scene	3D-LaneNet [7]	89.3	86.4	0.068	0.477	0.015	0.202
	Gen-LaneNet [8]	90.1	88.1	0.061	0.496	0.012	0.214
	CLGo [21]	94.2	91.9	0.061	0.361	0.029	0.250
	PersFormer [5]	-	92.9	0.054	0.356	0.010	0.234
	GP [16]	93.8	91.9	0.049	0.387	0.008	0.213
	Anchor3DLane [11]	97.2	95.6	0.052	0.306	0.015	0.223
	BEV-LaneDet [33]	-	98.7	0.016	0.242	0.020	0.216
	Ours	97.7	98.9	0.027	0.303	0.012	0.201
Rarely Observed	3D-LaneNet [7]	74.6	72.0	0.166	0.855	0.039	0.521
	Gen-LaneNet [8]	79.0	78.0	0.139	0.903	0.030	0.539
	CLGo [21]	88.3	86.1	0.147	0.735	0.071	0.609
	PersFormer [5]	-	87.5	0.107	0.782	0.024	0.602
	GP [16]	85.2	83.7	0.126	0.903	0.023	0.625
	Anchor3DLane [11]	96.9	94.4	0.094	0.693	0.027	0.579
	BEV-LaneDet [33]	-	99.1	0.031	0.594	0.040	0.556
	Ours	97.11	99.2	0.026	0.547	0.032	0.524
Visual Variations	3D-LaneNet [7]	74.9	72.5	0.115	0.601	0.032	0.230
	Gen-LaneNet [8]	87.2	85.3	0.074	0.538	0.015	0.232
	CLGo [21]	89.2	87.3	0.084	0.464	0.045	0.312
	PersFormer [5]	-	89.6	0.074	0.430	0.015	0.266
	GP [16]	92.1	89.9	0.060	0.446	0.011	0.235
	Anchor3DLane [11]	93.6	91.4	0.068	0.367	0.020	0.232
	BEV-LaneDet [33]	-	96.9	0.027	0.320	0.031	0.256
	Ours	96.4	97.1	0.032	0.317	0.022	0.235

Table 1. Performance comparison of state-of-the-art methods on the ApolloSim[8] dataset across three distinct split settings. "C" and "F" represent close and far ranges, respectively. Our model overall outperforms previous methods, particularly in rare and complex scenarios, demonstrating significant improvements in 3D lane detection accuracy and robustness

Method	F1(%)↑	Cate Acc(%)↑	x-Err/C(m)↓	x-Err/F(m)↓	z-Err/C(m)↓	z-Err/F(m)↓	FPS↑
3D-LaneNet [7]	44.1	-	0.479	0.572	0.367	0.443	53
Gen-LaneNet [8]	32.3	-	0.591	0.684	0.411	0.521	60
PersFormer [5]	50.5	92.3	0.485	0.553	0.364	0.431	21
Anchor3DLane [11]	54.3	90.7	0.275	0.310	0.105	0.135	87.3
BEV-LaneDet [33]	58.4	-	0.309	0.659	0.244	0.631	102
Ours	61.5	91.7	0.294	0.157	0.145	0.133	88

Table 2. Comparison of different 3D lane detection methods on the OpenLane dataset across various metrics. Our method achieves the highest accuracy and lowest localization errors, indicating superior lane detection performance.

achieves an AP of 97.11% and an F1 score of 99.2%. This robustness is further confirmed by our model’s minimal x-axis error in the far range (x-Err/F) of 0.547m and a reduced z-axis error (z-Err/F) of 0.524m, both of which are the lowest among all evaluated methods. These results highlight the resilience of Depth3DLane in scenarios that challenge depth and spatial perception, a key aspect of 3D lane detection.

In scenarios with visual variations, which introduce additional challenges due to lighting and environmental

changes, Depth3DLane maintains its advantage with an AP of 96.4% and an F1 score of 97.1%. Our model also minimizes x-axis errors far from the camera (x-Err/F), achieving 0.317m, the lowest across all methods tested. This precision, particularly under visually challenging conditions, suggests that Depth3DLane effectively retains contextual information and spatial accuracy, even with significant visual disturbances.

Method	All	Up & Down	Curve	Extreme Weather	Night	Intersection	Merge & Split
3D-LaneNet [7]	44.1	40.8	46.5	47.5	41.5	32.1	41.7
Gen-LaneNet [8]	32.3	25.4	33.5	28.1	18.7	21.4	31.0
PersFormer [5]	50.5	42.4	55.6	48.6	46.6	40.0	50.7
Anchor3DLane [11]	54.3	47.2	58.0	52.7	48.7	45.8	51.7
BEV-LaneDet [33]	58.4	48.7	63.1	53.4	53.4	50.3	53.7
Ours	61.5	50.3	63.9	54.2	54.1	51.4	54.5

Table 3. Per-scenario F1 score comparison on the OpenLane dataset, highlighting the robustness of our model across challenging conditions such as intersections, night-time, and extreme weather.

4.2.2. Results on OpenLane

Table 2 presents a quantitative comparison of our method against other baseline models across multiple metrics. Notably, our method achieved the highest AP and F1 scores, as well as the lowest x- and z-axis errors in both the close and far ranges. Specifically, our model reached an F1 score of 61.5%, surpassing the previous best model, BEV-LaneDet, by a significant margin. Furthermore, our model demonstrated superior accuracy in spatial localization, as indicated by the minimal x- and z-errors at far distances from the camera, reflecting improved robustness in depth and lateral position estimation.

Additionally, we performed a detailed breakdown of F1 scores across different scenarios within the OpenLane dataset, as shown in Table 3. Our method consistently outperformed previous approaches, particularly in challenging environments such as intersections, extreme weather, and night-time conditions. This enhanced performance can be attributed to our method’s improved capability to capture spatial relationships and effectively generalize across diverse environmental conditions. By addressing limitations found in prior methods and refining feature extraction through our model, our approach delivers a more robust and precise solution for monocular 3D lane detection in real-world driving scenarios.

4.3. Ablation Studies

In this section, we conduct ablation studies on OpenLane to analyze the impact of multi-scale feature alignment and key modules in our framework. The experiments evaluate different scale combinations for distillation and assess the contributions of the *Hierarchical Depth-Aware Head*, *Feature Distillation and Fusion*, and *Conditional Random Field* modules.

4.3.1. Multi-Scale Feature Alignment for Distillation

To investigate the impact of aligning features at different scales during the distillation process. Specifically, we experiment with aligning features at multiple scales to enhance the transfer of depth-related information across different levels of abstraction. The results, summarized in Ta-

ble 4, demonstrate that multi-scale feature alignment significantly boosts model performance.

Combination of scales	F-Score	z-Err/C(m)	z-Err/F(m)
S8	55.1	0.175	0.152
S16	59.0	0.167	0.165
S32	59.7	0.158	0.151
S64	59.1	0.157	0.156
S128	58.4	0.159	0.145
S32+S64	61.5	0.145	0.133
S32+S64+S128	60.9	0.152	0.131

Table 4. Comparison of different scale combinations in the depth prior distillation process. S8, S16, S32, S64, and S128 represent different levels of downsampling applied to the input image. For example, S32 corresponds to a 32x downsampling, while S32 + S64 refers to the concatenation of features from both 32x and 64x downsampled inputs. In addition to these scale combinations, we simultaneously activate two other key modules, utilizing the optimal combination to achieve the best performance in terms of F-Score and z-Error.

The experiments explore the following scale combinations:

- **Single Scale (S8, S16, S32, S64, S128):** Distilling depth priors from individual feature scales results in varying levels of improvement. For example, using the S32 scale yields the highest performance among single scales with an F-Score of 59.7.
- **Two-Scale Combination (S32 + S64):** Combining features from the S32 and S64 scales achieves the best F-Score of 61.5 and minimizes z-Error to 0.145, suggesting that deeper layers’ features are complementary to mid-level feature representations.
- **Three-Scale Combination (S32 + S64 + S128):** Adding the S128 scale to the S32 and S64 combination yields an F-Score of 60.9, with a slight increase in z-Error but a significant improvement in angular precision (z-Err/F(m) = 0.131).

The multi-scale fusion approach demonstrates that combining features from different layers at varying depths can

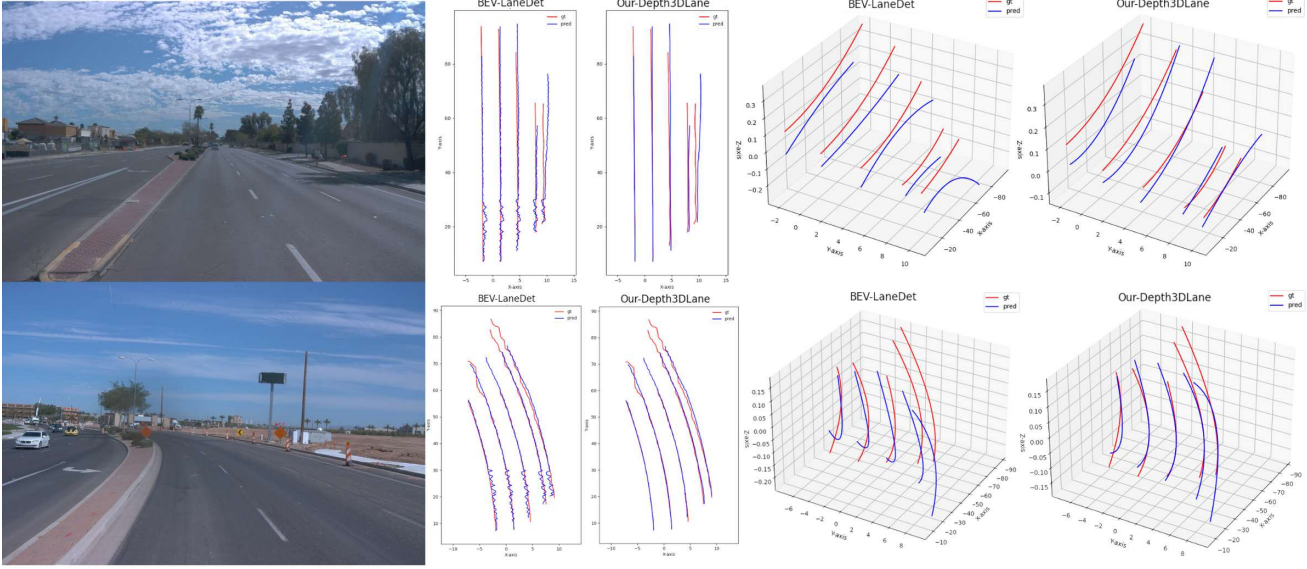


Figure 4. Qualitative comparison between our proposed Depth3DLane and BEV-LaneDet [33] on the OpenLane dataset. The first column shows the input images; the second column displays results from BEV-LaneDet in the Bird’s-Eye View (BEV); the third column illustrates our Depth3DLane model’s results in BEV; the fourth column presents BEV-LaneDet’s results in 3D space; and the fifth column depicts our model’s predictions in 3D space. It can be clearly observed that our Depth3DLane model significantly improves lane detection accuracy and continuity by effectively leveraging depth information for enhanced spatial perception, notably reducing localization errors, especially in the z-axis at far distances.

effectively capture both fine-grained details and more abstract depth representations, leading to improved overall depth estimation performance.

HDAH	FDAF	CRF	F-Score	z-Err/C	z-Err/F	FPS
✓			60.9	0.155	0.144	102
	✓		60.6	0.159	0.152	93
✓	✓		61.3	0.148	0.136	93
✓		✓	61.2	0.154	0.141	97
	✓	✓	60.9	0.152	0.139	88
✓	✓	✓	61.5	0.145	0.133	88

Table 5. Ablation study results for different module combinations. This study evaluates the impact of *Hierarchical Depth-Aware Head*, *Feature Distillation and Fusion*, and *Conditional Random Field* modules, evaluated by depth errors in close (z-Err/C) and far (z-Err/F) regions (m) and inference speed (FPS).

4.3.2. Three modules combination

To further understand the proposed modules, we evaluate the contributions of the *Hierarchical Depth-Aware Head* (HDAH), *Feature Distillation and Fusion* (FDAF), and *Conditional Random Field* (CRF) modules within the proposed framework. As illustrated in Table 5 we analyze their isolated and combined impacts:

- **HDAH**: Enhances depth feature extraction, achieving the highest standalone improvement with an F1-Score

of 60.2, significantly improving spatial awareness across varying road geometries.

- **FDAF**: Effectively transfers semantic depth knowledge and captures richer contextual information, reaching an F1-Score of 59.7 and showing its importance in depth feature refinement.
- **HDAH + FDAF**: Achieves robust depth alignment and complementary feature integration, resulting in an increased F1-Score of 61.2. This clearly demonstrates the importance of combining hierarchical depth extraction and semantic feature distillation.
- **HDAH + FDAF + CRF**: Results in the highest overall performance with an F1-Score of 61.5, further reducing errors and underscoring the effectiveness of spatial coherence enforced by the CRF module.

Overall, these results confirm the critical role and complementarity of the proposed modules, validating the effectiveness of our integration strategy.

5. Conclusion

In this paper, we propose Depth3DLane, a simple yet effective monocular 3D lane detection framework. We integrate a *Hierarchical Depth-Aware Head* to refine multi-scale depth features, mitigating inaccuracies of the flat-ground assumption. To enhance spatial accuracy, we employ *Feature Distillation and Fusion* to transfer depth knowledge from a pretrained model. Moreover, we introduce a *Conditional*

Random Field to enforce spatial coherence for robust lane predictions. Experimental results demonstrate that the combined application of these modules significantly surpasses each component individually, highlighting their complementary effectiveness. Our model achieves state-of-the-art performance across diverse driving scenarios, substantially reducing lane detection errors especially along the challenging z-axis at far distances. We believe our method can pave the way for future advancements in robust monocular-based 3D lane detection and autonomous driving applications.

References

- [1] Jianyong Ai, Wenbo Ding, Jiuhua Zhao, and Jiachen Zhong. Ws-3d-lane: Weakly supervised 3d lane detection with 2d lane labels. In *2023 IEEE International Conference on Robotics and Automation (ICRA)*, pages 5595–5601. IEEE, 2023. 2
- [2] Yifeng Bai, Zhirong Chen, Zhangjie Fu, Lang Peng, Pengpeng Liang, and Erkang Cheng. Curveformer: 3d lane detection by curve propagation with curve queries and attention. In *2023 IEEE International Conference on Robotics and Automation (ICRA)*, pages 7062–7068. IEEE, 2023. 2
- [3] Yifeng Bai, Zhirong Chen, Pengpeng Liang, and Erkang Cheng. Curveformer++: 3d lane detection by curve propagation with temporal curve queries and attention. *arXiv preprint arXiv:2402.06423*, 2024. 2
- [4] Durga Prasad Bavirisetti, Herman Ryen Martinsen, Gabriel Hanssen Kiss, and Frank Lindseth. A multi-task vision transformer for segmentation and monocular depth estimation for autonomous vehicles. *IEEE Open Journal of Intelligent Transportation Systems*, 2023. 3
- [5] Li Chen, Chonghao Sima, Yang Li, Zehan Zheng, Jiajie Xu, Xiangwei Geng, Hongyang Li, Conghui He, Jianping Shi, Yu Qiao, et al. Persformer: 3d lane detection via perspective transformer and the openlane benchmark. In *European Conference on Computer Vision*, pages 550–567. Springer, 2022. 2, 5, 6, 7
- [6] Michaël Fonder, Damien Ernst, and Marc Van Droogenbroeck. M4depth: Monocular depth estimation for autonomous vehicles in unseen environments. *arXiv preprint arXiv:2105.09847*, 2021. 3
- [7] Noa Garnett, Rafi Cohen, Tomer Pe’er, Roei Lahav, and Dan Levi. 3d-lanenet: end-to-end 3d multiple lane detection. In *Proceedings of the IEEE/CVF International Conference on Computer Vision*, pages 2921–2930, 2019. 2, 5, 6, 7
- [8] Yuliang Guo, Guang Chen, Peitao Zhao, Weide Zhang, Jinghao Miao, Jingao Wang, and Tae Eun Choe. Gen-lanenet: A generalized and scalable approach for 3d lane detection. In *Computer Vision—ECCV 2020: 16th European Conference, Glasgow, UK, August 23–28, 2020, Proceedings, Part XXI 16*, pages 666–681. Springer, 2020. 2, 5, 6, 7
- [9] Wencheng Han, Junbo Yin, and Jianbing Shen. Self-supervised monocular depth estimation by direction-aware cumulative convolution network. In *Proceedings of the IEEE/CVF International Conference on Computer Vision*, pages 8613–8623, 2023. 3
- [10] Kaiming He, Xiangyu Zhang, Shaoqing Ren, and Jian Sun. Deep residual learning for image recognition. In *Proceedings of the IEEE conference on computer vision and pattern recognition*, pages 770–778, 2016. 3, 4
- [11] Shaofei Huang, Zhenwei Shen, Zehao Huang, Zi-han Ding, Jiao Dai, Jizhong Han, Naiyan Wang, and Si Liu. Anchor3dlane: Learning to regress 3d anchors for monocular 3d lane detection. In *Proceedings of the IEEE/CVF Conference on Computer Vision and Pattern Recognition*, pages 17451–17460, 2023. 2, 3, 5, 6, 7
- [12] Dongkwon Jin, Wonhui Park, Seong-Gyun Jeong, Heeyeon

- Kwon, and Chang-Su Kim. Eigenlanes: Data-driven lane descriptors for structurally diverse lanes, 2022. 2
- [13] Nayeon Kim, Moonsub Byeon, Daehyun Ji, and Dokwan Oh. D-3dld: Depth-aware voxel space mapping for monocular 3d lane detection with uncertainty. In *ICASSP 2023-2023 IEEE International Conference on Acoustics, Speech and Signal Processing (ICASSP)*, pages 1–5. IEEE, 2023. 2
- [14] Yeongmin Ko, Younkwan Lee, Shoaib Azam, Farzeen Munir, Moongu Jeon, and Witold Pedrycz. Key points estimation and point instance segmentation approach for lane detection. *IEEE Transactions on Intelligent Transportation Systems*, 23(7):8949–8958, 2021. 2
- [15] John Lafferty, Andrew McCallum, Fernando Pereira, et al. Conditional random fields: Probabilistic models for segmenting and labeling sequence data. In *icml*, page 3. Williamstown, MA, 2001. 2
- [16] Chenguang Li, Jia Shi, Ya Wang, and Guangliang Cheng. Reconstruct from top view: A 3d lane detection approach based on geometry structure prior. In *Proceedings of the IEEE/CVF Conference on Computer Vision and Pattern Recognition (CVPR) Workshops*, pages 4370–4379, 2022. 6
- [17] Chenguang Li, Jia Shi, Ya Wang, and Guangliang Cheng. Reconstruct from top view: A 3d lane detection approach based on geometry structure prior. In *Proceedings of the IEEE/CVF Conference on Computer Vision and Pattern Recognition*, pages 4370–4379, 2022. 2
- [18] Xiang Li, Jun Li, Xiaolin Hu, and Jian Yang. Line-cnn: End-to-end traffic line detection with line proposal unit. *IEEE Transactions on Intelligent Transportation Systems*, 21(1): 248–258, 2019. 2
- [19] Zhuoling Li, Chunrui Han, Zheng Ge, Jinrong Yang, En Yu, Haoqian Wang, Xiangyu Zhang, and Hengshuang Zhao. Grouplane: End-to-end 3d lane detection with channel-wise grouping. *IEEE Robotics and Automation Letters*, 2024. 2
- [20] Ruijin Liu, Zejian Yuan, Tie Liu, and Zhiliang Xiong. End-to-end lane shape prediction with transformers. In *Proceedings of the IEEE/CVF winter conference on applications of computer vision*, pages 3694–3702, 2021. 2
- [21] Ruijin Liu, Dapeng Chen, Tie Liu, Zhiliang Xiong, and Zejian Yuan. Learning to predict 3d lane shape and camera pose from a single image via geometry constraints. In *Proceedings of the AAAI Conference on Artificial Intelligence*, pages 1765–1772, 2022. 2, 6
- [22] Yueru Luo, Chaoda Zheng, Xu Yan, Tang Kun, Chao Zheng, Shuguang Cui, and Zhen Li. Latr: 3d lane detection from monocular images with transformer. In *Proceedings of the IEEE/CVF International Conference on Computer Vision*, pages 7941–7952, 2023. 2
- [23] Fulong Ma, Weiqing Qi, Guoyang Zhao, Linwei Zheng, Sheng Wang, Yuxuan Liu, and Ming Liu. Monocular 3D lane detection for Autonomous Driving: Recent Achievements, Challenges, and Outlooks. 2
- [24] Chaesong Park, Eunbin Seo, and Jongwoo Lim. Heightlane: Bev heightmap guided 3d lane detection. *arXiv preprint arXiv:2408.08270*, 2024. 2
- [25] Zhan Qu, Huan Jin, Yang Zhou, Zhen Yang, and Wei Zhang. Focus on local: Detecting lane marker from bottom up via key point. In *Proceedings of the IEEE/CVF conference on computer vision and pattern recognition*, pages 14122–14130, 2021. 2
- [26] Olaf Ronneberger, Philipp Fischer, and Thomas Brox. U-net: Convolutional networks for biomedical image segmentation. In *Medical image computing and computer-assisted intervention–MICCAI 2015: 18th international conference, Munich, Germany, October 5–9, 2015, proceedings, part III 18*, pages 234–241. Springer, 2015. 2, 3
- [27] Pei Sun, Henrik Kretzschmar, Xerxes Dotiwalla, Aurelien Chouard, Vijaysai Patnaik, Paul Tsui, James Guo, Yin Zhou, Yuning Chai, Benjamin Caine, et al. Scalability in perception for autonomous driving: Waymo open dataset. In *Proceedings of the IEEE/CVF conference on computer vision and pattern recognition*, pages 2446–2454, 2020. 5
- [28] Lucas Tabelini, Rodrigo Berriel, Thiago M Paixao, Claudine Badue, Alberto F De Souza, and Thiago Oliveira-Santos. Keep your eyes on the lane: Real-time attention-guided lane detection. In *Proceedings of the IEEE/CVF conference on computer vision and pattern recognition*, pages 294–302, 2021. 2
- [29] Lucas Tabelini, Rodrigo Berriel, Thiago M Paixao, Claudine Badue, Alberto F De Souza, and Thiago Oliveira-Santos. Polyplanenet: Lane estimation via deep polynomial regression. In *2020 25th International Conference on Pattern Recognition (ICPR)*, pages 6150–6156. IEEE, 2021. 2
- [30] Wouter Van Gansbeke, Bert De Brabandere, Davy Neven, Marc Proesmans, and Luc Van Gool. End-to-end lane detection through differentiable least-squares fitting. In *Proceedings of the IEEE/CVF International Conference on Computer Vision Workshops*, pages 0–0, 2019. 2
- [31] Jinsheng Wang, Yinchao Ma, Shaofei Huang, Tianrui Hui, Fei Wang, Chen Qian, and Tianzhu Zhang. A keypoint-based global association network for lane detection. In *Proceedings of the IEEE/CVF Conference on Computer Vision and Pattern Recognition*, pages 1392–1401, 2022. 2
- [32] Jinsheng Wang, Yinchao Ma, Shaofei Huang, Tianrui Hui, Fei Wang, Chen Qian, and Tianzhu Zhang. A keypoint-based global association network for lane detection, 2022. 5
- [33] Ruihao Wang, Jian Qin, Kaiying Li, Yaochen Li, Dong Cao, and Jintao Xu. Bev-lanedet: An efficient 3d lane detection based on virtual camera via key-points. In *Proceedings of the IEEE/CVF Conference on Computer Vision and Pattern Recognition*, pages 1002–1011, 2023. 1, 2, 3, 4, 5, 6, 7, 8
- [34] Lihe Yang, Bingyi Kang, Zilong Huang, Xiaogang Xu, Jiashi Feng, and Hengshuang Zhao. Depth anything: Unleashing the power of large-scale unlabeled data. In *Proceedings of the IEEE/CVF Conference on Computer Vision and Pattern Recognition*, pages 10371–10381, 2024. 3
- [35] Lihe Yang, Bingyi Kang, Zilong Huang, Zhen Zhao, Xiaogang Xu, Jiashi Feng, and Hengshuang Zhao. Depth anything v2. *arXiv preprint arXiv:2406.09414*, 2024. 2, 3, 4, 5
- [36] Tu Zheng, Yifei Huang, Yang Liu, Wenjian Tang, Zheng Yang, Deng Cai, and Xiaofei He. Clrnet: Cross layer refinement network for lane detection. In *Proceedings of the IEEE/CVF conference on computer vision and pattern recognition*, pages 898–907, 2022. 2